RAFFLES BULLETIN OF ZOOLOGY **66**: 394–401
Date of publication: 29 June 2018
http://zoobank.org/urn:lsid:zoobank.org:pub:4E5652B3-9B8E-4735-8C86-A0EFA964C7EF

Notes on egg structure and larval development in the highly miniaturised and progenetic *Paedocypris* (Teleostei: Cyprinidae)

Kevin W. Conway[1*], Olivier Perrin[2] and Ralf Britz[3]

Abstract. Egg structure and larval development of *Paedocypris carbunculus* are described based on 15 specimens (2 eggs, 13 larvae) obtained from captive rearing. The adhesive eggs, which are laid on the underside of plant leaves, are 450–500 µm in diameter with a smooth surface. Eggs hatch ca. 36 hours after egg deposition, and newly hatched larvae measure ca.1.6 mm. Larvae attach to the substrate using a gular adhesive organ, comprising a concave central depression surrounded by a low semi-circular ridge of elevated epidermal cells. The yolk sac is fully resorbed by 2.1 mm NL. The swimbladder is present by 2.0 mm NL and is divided into anterior and posterior chambers by 4.1 mm SL, which become widely separate and connected via a short duct by 5.3 mm SL. Flexion occurs by 4.0 mm SL. The sequence of fin ray formation is caudal>anal>dorsal>pectoral>pelvic. Adult fin ray counts and pigmentation are present by 7.6 mm SL.

Key words. ontogeny, miniaturisation, zebrafish

INTRODUCTION

The genus *Paedocypris* Kottelat, Britz, Tan & Witte, 2006 is endemic to the highly acidic peat swamp forests of Sundaland (Kottelat et al., 2006; Britz & Kottelat, 2008). Maturing at sizes between 7.9–8.8 mm SL and attaining maximum sizes of 10–11.5 mm SL, the three highly miniaturised species of *Paedocypris* are considered to represent the world's smallest species of vertebrates (Kottelat et al., 2006; Rüber et al., 2007; though see Rittmeyer et al., 2012). Adults of *Paedocypris* are transparent, retain the precaudal larval-fin fold and bear an overall resemblance to the larvae of close relatives (Kottelat et al., 2006). The external larval appearance of mature *Paedocypris* is mirrored by their internal skeletal anatomy, which is greatly simplified and characterised by a large number of absences (Britz & Conway, 2009) hypothesised to be the result of organism-wide progenetic paedomorphosis via developmental truncation (Britz et al., 2014; Britz & Conway, 2016). The genome of *Paedocypris* is also characterised by reduction, including an overall lower DNA content and reduced karyotype with a lower number of chromosomes compared to that of close relatives (Liu et al., 2012; Malmstrøm et al., 2018) including the absence of multiple homeobox (HOX) genes and other genes important during development (Malmstrøm et al., 2018).

In stark contrast to this overall theme of reduction and simplification, *Paedocypris* exhibits a number of highly derived sexual dimorphisms that involve enlargement or hyperossification of skeletal elements, including (in males) highly modified pelvic-fin rays and a hypertrophied pelvic girdle, elongate pectoral-fin rays and a more heavily ossified pectoral girdle, a more heavily ossified outer arm of the os suspensorium, and (in females) a more heavily ossified first proximal-middle radial supporting the anteriormost dorsal-fin rays (Kottelat et al., 2006; Britz & Conway, 2009). These features were initially suspected to play a role in reproduction (Kottelat et al., 2006; Britz & Conway, 2009) and these suspicions were confirmed in part via observations on spawning events of *Paedocypris carbunculus* Britz & Kottelat, 2008 maintained in aquaria (Britz & Kottelat, 2008; Perrin & Beyer, 2008). These successful spawning events not only provided an opportunity to observe aspects of courtship and egg laying in *Paedocypris* but also an opportunity to obtain and study early developmental stages. In the present paper we describe the eggs and larval stages of *Paedocypris* based on material raised in aquaria by the second author (OP).

MATERIAL & METHODS

A group of *Paedocypris carbunculus* were maintained and successfully bred in a 30 litre aquarium, with the following water condition: pH 4–5, conductivity 20–100 µS/cm^{-1}, and temperature 27°C. See Perrin & Beyer (2008) for details on general maintenance and conditioning for spawning. Eggs and newly hatched larvae were photographed in the aquarium using a Nikon D200 with macro lens and extension tubes. Select eggs and larvae from successful spawning events were fixed in 10% buffered formalin and transferred to 70% ethanol for permanent storage. Specimens were examined

[1]Department of Wildlife and Fisheries Sciences and Biodiversity Research and Teaching Collections, Texas A&M University, College Station, TX 77843, USA; Email: kevin.conway@tamu.edu (*corresponding author)

[2]13 rue Germain Pilon, 75018, Paris, France

[3]Department of Zoology, Natural History Museum, Cromwell Road, London, SW7 5BD, UK

ISSN 2345-7600 (electronic) | ISSN 0217-2445 (print)

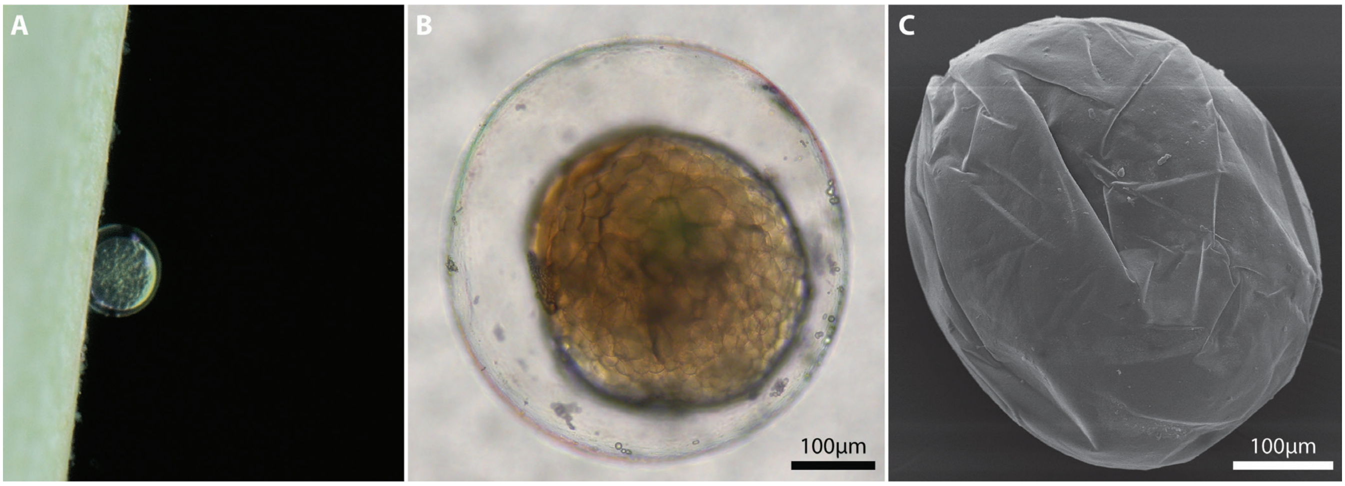

Fig. 1. Eggs of *Paedocypris carbunculus*. A, Recently laid egg attached to underside of plant leaf in aquarium (photograph by O. Perrin); B, Light microscope; C, SEM.

using a ZEISS SteREO Discovery V20 Microscope and photographed using a ZEISS AxioCam MRc5 digital camera attached to the aforementioned microscope. Stacked images were processed using Adobe Photoshop CS5.1 and Adobe Illustrator CS5.1. A single egg and larva (1.6 mm SL) were initially dehydrated using a graded series of ethanol, critical point dried (Denton DCP-1A), placed on an aluminum stub and coated with gold (Denton Desk IV XLS) for examination with scanning electron microscopy (SEM) using a Philips XL-20 SEM. Colour pattern terminology follows Britz & Kottelat (2008).

Material examined is deposited in the Natural History Museum, London (BMNH): BMNH 2018.6.20.1-15, 15 (including 2 eggs); ca. 450µm–7.6 mm SL. — BMNH 2008.4.14.2–26, paratypes, 25; 6.2–11.5 mm SL.

RESULTS

Eggs. The spherical eggs (n=2) measure 450–500 µm in diameter, with a relatively large (ca. 400 µm) yolk occupying the majority of the internal space of the egg (Fig. 1A, B). The egg surface appears smooth under SEM at low magnification (Fig. 1C). The micropyle could not be located. Embryonic development was not observed.

Larvae and juveniles. Eggs hatch ca. 36 hrs after deposition (Perrin & Beyer, 2008). Newly hatched larvae measure ca. 1.6 mm NL and exhibit a large yolk-sac that extends posteriorly along the ventral midline giving the yolk-sac a triangular appearance in ventral view (Fig. 2A). A larval-fin fold extends along the entire dorsal surface of the body around the tail region to the anus. A large pre-anal fin fold extends from the anus to the posterior margin of the yolk sac. The newly hatched larvae adhere to the substrate via an attachment organ located at the gular region (Fig. 2B). The attachment organ exhibits a central concavity surrounded anterolaterally by a low, semi-circular ridge (Fig. 2B). The ridge of the attachment organ appears white in fixed specimens. Surface micro-features of the cells contributing to the attachment organ were difficult to observe under SEM due to the presence of a fibrous, potentially adhesive material scattered over the surface of the organ (Fig. 2C). Using the adhesive organ, larvae attach to the substrate for several hours after hatching (Fig. 2A; Perrin & Beyer, 2008).

In the smallest preserved larva available for study (1.7 mm NL; Fig. 3A), the yolk-sac is circular (without posterior extension) and the pectoral-fin buds are already well developed. The gut is a short, sigmoid tube running dorsal and posterior to the yolk-sac, which is fully resorbed in specimens ≥ 2.1 mm NL. The swim bladder is first recognisable as a small sac dorsal to the yolk-sac in a larva 2.0 mm NL and is divided into anterior and posterior chambers in specimens ≥ 4.2 mm SL (Fig. 3B–G; Table 1). By 4.2 mm SL (Fig. 3B), flexion has occurred and multiple caudal-fin rays are supported by the parhypural and five hypural cartilages. Anal-fin rays are developing by 4.6 mm SL (Fig. 3C). Dorsal-fin rays are present by 5.0 mm SL (Fig 3D). Pectoral-fin rays have appeared by 5.3 mm SL. The larval-fin fold is completely resorbed anterior to the dorsal fin by 5.3 mm SL and the post-dorsal and post-anal fin portions of the fold have regressed to reveal the outline of the three median fins (Fig. 3E). Tiny pelvic-fin buds are first visible at 5.3 mm SL as tiny flap-like structures straddling the pre-anal larval-fin fold on the ventral surface of the body mid-way between the gill openings and the anus (Fig. 3E). The anterior and posterior chambers of the swimbladder are separated by 5.3 mm SL but connected via a short tube.

By 6.0 mm SL the post-dorsal portion of the larval-fin fold is almost completely resorbed and the post-anal portion is free from the posterior margin of the anal fin (Fig. 3F). By 6.7 mm SL, the pre- and post-anal larval-fin folds are identical to the adult condition. By 7.6 mm SL, the full complement of fin rays is present and the appearance is overall that of the adult (Fig. 3G). At this size, the majority of the rays are still unbranched, with only very few branched rays in the dorsal and anal fins (Table 1).

Features of larval pigmentation are provided in Table 2. In the smallest larvae available for study (1.7–2.1 mm NL; Fig.

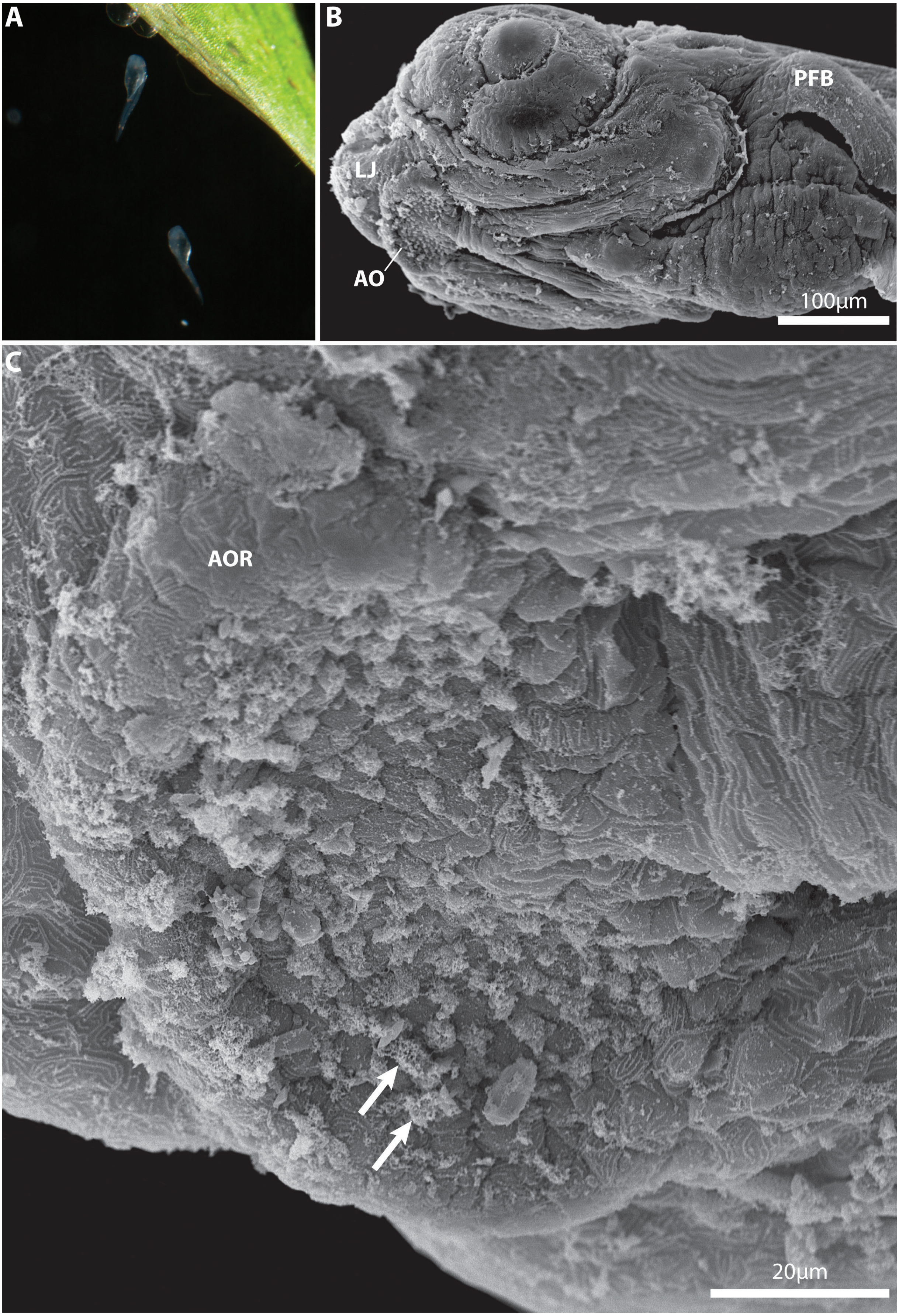

Fig. 2. Adhesion and adhesive organ in larvae of *Paedocypris carbunculus*. A, Recently hatched larvae adhering to aquarium side (photograph by O. Perrin); B, SEM of head and anterior part of body in ventrolateral view, anterior to right, highlighting position of adhesive organ in gular region (BMNH 2018.6.20.1-15, ca. 1.6 mm NL); C, SEM close up of adhesive organ, anterior to left. White arrows in C indicate fibrous material on surface of adhesive organ. Abbreviations: AO, adhesive organ; AOR, adhesive organ ridge; LJ, lower jaw; PFB, pectoral-fin bud.

Fig. 3. Larvae (A–F) and juvenile (G) stages of *Paedocypris carbunculus* (BMNH 2018.6.20.1-15), right side, lateral view. A, 1.7 mm NL; B, 4.2 mm SL; C, 4.6 mm SL; D, 5.0 mm SL; E, 5.3 mm SL; F, 6.0 mm SL; G, 7.6 mm SL. White arrows in E and F point to pelvic-fin bud.

3A, Table 2), the most prominent features of pigmentation are restricted to the dorsal and ventral midlines. This includes the middorsal stripe and paired ventrolateral rows, which are located along the junction of the larval-fin fold and the body musculature, a prominent chest blotch on the ventral surface of the yolk sac, and a concentration of melanophores on the dorsal and ventral surface of the head, likely corresponding to the posterior head blotch and gular pigment present in adults. Additional melanophores also line the surface of the viscera and the head kidney. At a point corresponding to roughly one head length anterior to the posterior tip of the notochord, the melanophores contributing to the middorsal and paired ventrolateral rows of the smallest larvae are visible in lateral view as a pair of conspicuous dark brown streaks. This feature is absent from larger specimens and may be specific to yolk-sac stage larvae. The smallest post-flexion larvae available for study (4.2–4.3 mm SL; Fig. 3B, Table 2) exhibit pigmentation on the snout and lips and

Table 1. Select morphological features for 11 larvae and 1 juvenile specimen (7.6 mm SL) of *Paedcypris carbunculus*. Counts for fin rays (excluding caudal-fin rays) include the total number of rays present followed by the number of unbranched (lower case Roman numerals) and unbranched rays (Arabic numerals). Counts for caudal-fin rays include the total number of principal rays (upper+lower lobe)/dorsal+ventral procurrent rays. Abbreviations AC and PC refer to the anterior- and posterior chambers, respectively, of the swimbladder.

Specimen length (NL/SL)	Yolk Sac	Gut	Swimbladder	Dorsal Fin	Anal Fin	Caudal Fin	Pectoral Fin	Pelvic Fin
1.7 mm NL (Fig. 3A)	Spherical	Straight tube	–	–	–	–	–	–
2.0 mm NL	Spherical	Sigmoid; sac-like anterior chamber; straight tube posteriorly	Single chamber	–	–	–	–	–
2.1 mm NL	Spherical	Sigmoid; sac-like anterior chamber; straight tube posteriorly	Single chamber	–	–	–	Bud only	–
4.2 mm SL (Fig. 3B)	–	Sac-like anterior chamber ventral to PC; straight tube posteriorly	AC and PC equal in size; in contact	–	–	10	Bud only	–
4.3 mm SL	–	Sac-like anterior chamber ventral to PC; straight tube posteriorly	AC and PC equal in size; in contact	–	–	11	Bud only	–
4.6 mm SL (Fig. 3C)	–	Sac-like anterior chamber ventral to PC; straight tube posteriorly	AC and PC equal in size; in contact	–	5 (v)	15 (8+7)	Bud only	–
5.0 mm SL (Fig. 3D)	–	Sac-like anterior chamber ventral to PC; straight tube posteriorly	AC and PC equal in size; in contact	3(iii)	7(viii)	15 (8+7)/1+1	Bud only	–
5.3 mm SL (Fig 3E)	–	Sac-like anterior chamber ventral to PC; straight tube posteriorly	PC larger than AC; separated by a short duct	4 (iiii)	10 (x)	16 (8+8)/1+1	3 (iii)	Tiny bud only
6.0 mm SL (Fig. 3F)	–	Sac-like anterior chamber ventral to PC; straight tube posteriorly	As adult	7 (vii)	11 (xi)	Damaged	5 (v)	Tiny bud only
6.7 mm SL	–	Only intestine visible; straight	As adult	7 (vii)	11 (xi)	15 (8+7)/3+2	6 (vi)	1 (i)
7.0 mm SL	–	Only intestine visible; straight	As adult	7 (iii, 1, iii)	11 (xi)	16 (8+8)/3+2	6 (vi)	2 (ii)
7.6 mm SL (Fig. 3G)	–	Only intestine visible; straight	As adult	7 (iii, 1, iii)	10 (iiii, 3, iii)	16 (8+8)/4+2	6 (vi)	5 (v)

Table 2. Pigmentation in larvae (n=11; 1.7–7.0 mm NL/SL), juvenile (n=1; 7.6 mm SL) and adult (n=1; 9.7 mm SL) specimens of *Paedocypris carbunculus*. Terminology follows that of Britz & Kottelat (2008) excluding paired streaks along base of tail.

	Specimen Length (NL/SL)												
Pigmentation Component	1.7 mm NL (Fig. 3A)	2.0 mm NL	2.1 mm NL	4.2 mm SL (Fig. 3B)	4.3 mm SL	4.6 mm SL (Fig. 3C)	5.0 mm SL (Fig. 3D)	5.3 mm SL (Fig. 3E)	6.0 mm SL (Fig. 3F)	6.7 mm SL	7.0 mm SL	7.6 mm SL (Fig. 3G)	9.7 mm SL
Paired streaks along base of tail	×	×	×	–	–	–	–	–	–	–	–	–	–
Middorsal stripe	×	×	×	×	×	×	×	×	×	×	×	×	×
Ventrolateral row	×	×	×	×	×	×	×	×	×	×	×	×	×
Preanal pigmentation	×	×	×	×	×	×	×	×	×	×	×	×	×
Chest blotch	×	×	×	×	×	×	×	×	×	×	×	×	×
Posterior head blotch	×	×	×	×	×	×	×	×	×	×	×	×	×
Gular pigmentation	×	×	×	×	×	×	×	×	×	×	×	×	×
Head kidney pigment	×	×	×	×	×	×	×	×	×	×	×	×	×
Midlateral row	–	–	–	×	×	×	×	×	×	×	×	×	×
Swimbladder row	–	–	–	×	×	×	×	×	×	×	×	×	×
Ventrolateral abdominal pigment	–	–	–	×	×	×	×	×	×	×	×	×	×
Branchiostegal rows	–	–	–	×	×	×	×	×	×	×	×	×	×
Isthmus pigment	–	–	–	×	×	×	×	×	×	×	×	×	×
Anterior head blotch	–	–	–	–	–	×	×	×	×	×	×	×	×
Opercular, subopercular and preopercular rows	–	–	–	–	–	×	×	×	×	×	×	×	×
Anal-fin base	–	–	–	–	–	–	×	×	×	×	×	×	×
Chest spots	–	–	–	–	–	–	–	–	–	×	×	×	×
Postotic row	–	–	–	–	–	–	–	–	–	×	×	×	×
Larval fin-fold row	–	–	–	–	–	–	–	–	–	–	–	–	×

additional pigment on the ventral and ventrolateral surface of the head (isthmus pigment and branchiostegal rows). The midlateral row is represented by a series of widely spaced melanophores along the horizontal septum. An extensive sheet of melanophores also caps the dorsal surface of the swimbladder (Fig. 3B). Small dark brown melanophores also are scattered across the surface of the caudal-fin rays and the membranes in between the rays. By 6.7 mm SL, pigmentation is similar to that of the adult (Table 2; Fig. 3F,G) differing only by the absence of the larval-fin fold row of melanophores.

DISCUSSION

Our study is the first to look at the external development of selected stages of *Paedocypris*, but admittedly our sample size is quite limited in terms of stages and specimens with the largest gap in our series between the yolk sac stage and the stage when the caudal-fin rays have started to form. Despite these limitations, a comparison of the development of external features in *P. carbunculus* with that of zebrafish *Danio rerio* yields interesting details.

Eggs of *P. carbunculus* are adhesive and hatch after 36 h, whereas those of *D. rerio* are non-adhesive and begin hatching at about 48 h post fertilisation (range 48–72 h; Nüsslein-Volhard & Dahm, 2002). Larvae of *Paedocypris* attach to the substrate after hatching and can be seen hanging on the glass of the aquarium until the yolk sac is resorbed. Attachment is achieved with the aid of a complex multicellular attachment organ on the gular area of the head and can be assigned to Ilg's (1952) type 2 of teleost attachment organs. Larvae of *Danio*, though also with adhesive abilities, lack such an organ and seem to rely on scattered attachment cells in the head epidermis, the type 1 organ of Ilg (1952). Larval attachment organs are poorly studied in cyprinids, but have been reported from *Devario* (Jones, 1938; Ilg, 1952; Britz, 2002) and *Pethia* (Britz, 2002). Larval *Devario* have a multicellular attachment organ on top of the head, unlike the gular organ in *Paedocypris*, and that of *Pethia* consists of scattered attachment cells on the front of the head and along the margin of the upper lip. Even considering the diversity of attachment organs among teleosts (Peters & Berns, 1982; Britz, 1997, 2002; Britz et al., 2000; Britz & Cambray, 2001), the gular adhesive organ of *Paedocypris* seems to be unique and another autapomorphy of this taxon.

After resorption of the yolk sac, subsequent external development is similar to that reported for other Asian cyprinids such as *Danio* (Parichy et al., 2009), *Devario* (Sado & Kimura, 2006) or *Tanichthys* (Sado & Kimura, 2005b), in that the sequence of fin ray formation is: caudal >anal>dorsal>pectoral>pelvic. There is variation in the sequence of fin ray formation across Cyprinidae and in some taxa dorsal- and anal-fin rays appear simultaneously (i.e., caudal>dorsal/anal>pectoral>pelvic as in *Richardsonius balteatus*, *Notemigonus crysoleucas* [Snyder et al., 2016], *Acheilognathus limbata* [Suzuki & Jeon, 1988], *Horadandia* [Sado & Kimura, 2005a] or *Barbus trevelyani* [Cambray, 1985]) or the dorsal-fin rays develop earlier than the anal-fin rays (i.e., caudal>dorsal>anal>pectoral>pelvic as in *Cyprinella lutrensis*, *Cyprinus carpio*, *Rhinichthys cataractae* [Snyder et al., 2016], *Pseudogobio esocinus* [Nakajima & Onikura, 2015], *Hypsibarbus malcolmi* [Ogata et al., 2010] or *Barbus anoplus* [Cambray, 1983]). The latter sequence, which appears to be most common amongst the cyprinids for which information on larval development is available, is also present in the Catostomidae (Hogue & Buchanan, 1977; Buynak & Mohr, 1978) and may represent the plesiomorphic condition for Cypriniformes. Deciphering which of these alternative sequences of fin ray formation are apomorphic or plesiomorphic is beyond the scope of this study and would require additional information on larval development in members of the other cypriniform groups and basal members from other groups of otophysans.

The majority of unusual morphological characters of *Paedocypris* are restricted to the skeleton and further study is needed to determine whether skeletal development of *Paedocypris* shows unusual features or follows the typical ontogenetic trajectory of cyprinids, as exemplified by the zebrafish *D. rerio* (Cubbage & Mabee, 1995; Bird & Mabee 2003).

ACKNOWLEDGEMENTS

We thank D. Siegel and D. Sever for help with SEM at Southeastern Louisiana University, K. Kubicek and D. Kim for help locating literature, and K. Kubicek for comments on an earlier draft of the manuscript. KWC acknowledges financial support from Texas A&M AgriLife Research (TEX09452). This is publication #1573 of the Biodiversity Research and Teaching Collections of Texas A&M University.

LITERATURE CITED

Bird NC & Mabee PM (2003) Developmental morphology of the axial skeleton of the zebrafish, *Danio rerio* (Ostariophysi: Cyprinidae). Developmental Dynamics, 228(3): 337–357.

Britz R (1997) Egg surface structure and larval cement glands in nandid and badid fishes with remarks on phylogeny and zoogeography. American Museum Novitates, 3195: 1–17.

Britz R (2002) Larvale Anheftungsorgane bei Teleostei. In: Greven H & Riehl R (eds.) Verhalten der Aquarienfische (2). Birgit Schmettkamp Verlag, Bornheim. Pp. 17–35.

Britz R & Cambray JA (2001) Structure of egg surfaces and attachment organs in anabantoids. Ichthyological Exploration of Freshwaters, 12(3): 267–288.

Britz R & Conway KW (2009) Osteology of *Paedocypris*, a miniature and highly developmentally truncated fish (Teleostei: Ostariophysi: Cyprinidae). Journal of Morphology, 270(4): 389–412.

Britz R & Conway KW (2016) *Danionella dracula*, an escape from the cypriniform *Bauplan* via developmental truncation? Journal of Morphology, 277: 147–66.

Britz R, Conway KW & Rüber L (2014) Miniatures, morphology and molecules: *Paedocypris* and its phylogenetic position (Teleostei, Cypriniformes). Zoological Journal of the Linnean Society, 172(3): 556–615.

Britz R, Kirschbaum F & Heyd A (2000) Observations on the structure of larval attachment organs in three species of gymnotiforms (Teleostei: Ostariophysi). Acta Zoologica, 81(1): 57–67.

Britz R & Kottelat M (2008) *Paedocypris carbunculus*, a new species of miniature fish from Borneo (Teleostei: Cypriniformes: Cyprinidae). Raffles Bulletin of Zoology, 56(2): 415–422.

Buynak GL & Mohr JR HW (1978) Larval development of the northern hog sucker (*Hypentelium nigricans*), from the Susquehanna River. Transactions of the American Fisheries Society, 107(4): 595–599.

Cambray JA (1983) Early development and larval behaviour of a minnow, *Barbus anoplus* (Pisces: Cyprinidae). South African Journal of Zoology, 18(4): 331–336.

Cambray JA (1985) Early development of an endangered African barb, *Barbus trevelyani* (Pisces: Cyprinidae). Revue d'Hydrobiologie Tropicale, 18(1): 51–60.

Cubbage CC & Mabee PM (1996) Development of the cranium and paired fins in the zebrafish *Danio rerio* (Ostariophysi, Cyprinidae). Journal of Morphology, 229(2): 121–160.

Ilg L (1952) Über larvale Haftorgane bei Teleosteern. Zoologische Jahrbücher, Abteilung für Anatomie und Ontogenie der Tiere, 72: 577–600.

Hogue Jr JJ & Buchanan JP (1977) Larval development of spotted sucker (*Minytrema melanops*). Transactions of the American Fisheries Society, 106(4): 347–353.

Jones S (1938) On the breeding habits and development of a cyprinid, *Danio (Danio) malabaricus* (Jerdon) in Ceylon. Ceylon Journal of Science Section C, 6: 79–89.

Kottelat M, Britz R, Tan HH & Witte KE (2006) *Paedocypris*, a new genus of Southeast Asian cyprinid fish with a remarkable sexual dimorphism, comprises the world's smallest vertebrate. Proceedings of the Royal Society of London B, 273: 895–899.

Liu S, Tan HH, Tan SL & Hong Y (2012) Chromosome evolution and genome miniaturization in minifish. PloS one, 7(5): e37305.

Malmstrøm M, Britz R, Matschiner M, Tørresen OK, Hadiaty RK, Yaakob N, Tan HH, Jakobsen KS, Salzburger W & Rüber L (2018) The most developmentally truncated fishes show extensive *Hox* gene loss and miniaturized genomes. Genome Biology and Evolution, 10(4): 1088–1103. DOI: https://doi.org/10.1101/160168.

Nakajima J & Onikura N (2015) Larval and juvenile development of Pike Gudgeon, *Pseudogobio esocinus* (Cyprinidae: Gobioninae). Ichthyological Research, 62(3): 268–273.

Nüsslein-Volhard C & Dahm R (2002) Zebrafish: A Practical Approach. Oxford University Press, New York. 303 pp.

Ogata Y, Morioka S, Sano K, Vongvichith B, Eda H, Kurokura H & Khonglaliane T (2010) Growth and morphological development of laboratory-reared larvae and juveniles of the Laotioan indigenous cyprinid *Hypsibarbus malcolmi*. Ichthyological Research, 57(4): 389–397.

Parichy DM, Elizondo MR, Mills MG, Gordon TN & Engeszer RE (2009) Normal table of postembryonic zebrafish development: Staging by externally visible anatomy of the living fish. Developmental Dynamics, 238(12): 2975–3015.

Perrin O & Beyer P (2008) Das komplexe Liebesleben des ''Roten *Paedocypris*'' von Borneo I. Die Aquarien- und Terrarienzeitschrift, 61(1): 24–29.

Peters HM & Berns S (1982) Die Maulbrutpflege der Cichliden. Untersuchungen eines Verhaltensmusters. Zeitschrift für Zoologische Systematik und Evolutionsforschung, 20: 18–52.

Rittmeyer EN, Allison A, Gründler MC, Thompson DK & Austin CC (2012) Ecological guild evolution and the discovery of the world's smallest vertebrate. PLoS one, 7(1): e29797.

Rüber L, Kottelat M, Tan HH, Ng PK & Britz R (2007) Evolution of miniaturization and the phylogenetic position of *Paedocypris*, comprising the world's smallest vertebrate. BMC Evolutionary Biology, 7(1): 38.

Sado T & Kimura S (2005a) Developmental morphology of the cyprinid fish *Horadandia atukorali*. Ichthyological Research, 52(2): 152–157.

Sado T & Kimura S (2005b) Developmental morphology of the cyprinid fish *Tanichthys albonubes*. Ichthyological Research, 52(4): 386–391.

Sado T & Kimura S (2006) Developmental morphology of the cyprinid fish *Inlecypris auropurpureus*. Ichthyological Research, 53(1): 34–40.

Snyder DE, Seal SC, Charles JA & Bjork CL (2016) Cyprinid Fish Larvae and Early Juveniles of the Upper Colorado River Basin — Morphological Descriptions, Comparisons, and Computer-Interactive Key. Colorado Parks and Wildlife Technical Publication 47, Colorado Parks and Wildlife, 208 pp.

Suzuki N & Jeon S-R (1988) Development of the bitterling, *Acheilognathus limbata* (Cyprinidae) from Korea and Japan, with notes on minute tubercles on the skin surface and on genetic implication in hybrid embryos. Korean Journal of Limnology, 21: 211–299.